Controlled Synthesis of Novel Chromium Nitride Dendritic and Bundle-like Nanocrystals via Solvent-free Route at Low Temperature

Wei Luo, Fei Zheng, Kun Zhu, Xiaobo Tian, and Yi Xie*
*Nano-materials and Nano-chemistry, Hefei National Laboratory for Physical Sciences at Microscale,
Department of Chemistry, University of Science and Technology of China, Hefei, Anhui 230026, P. R. China*

By controlling the supersaturation, cubic CrN with novel dendritic and bundle-like nanostructures was synthesized via the solvent-free reaction of $CrCl_3$ and $NaNH_2$ at 250 °C. On the basis of the characterization of the obtained products by XRD, XPS, TEM, HRTEM, and FESEM, the possible formation mechanism of CrN with different nanostructures is proposed here.

Figure 1. XRD pattern of as-obtained CrN dendrites.

Recently, there has been increasing interest in materials with specific nanostructures because of the expectation of novel properties. Dendritic nanostructures are one type of attractive supra-molecular structures, and in the decades, a variety of methods have been used to prepare nanodendrites.[1] Although chromium nitride is of particular interest in the electronics industry owing to its high hardness and low electrical resistivity, limited methods[2] have been developed, and few nanostructures have been reported, except for nanoparticles. Hence, the synthesis of additional types of nanostructures is highly desired and potentially technologically important. Herein, we describe a synthetic method that leads to novel dendritic and bundle-like CrN nanostructures at low temperature. To our knowledge, it is the first time to obtain pure cubic CrN with novel dendritic nanostructures.

All manipulations were performed in a N_2 flow glove box to avoid the effect of the oxygen and moisture. In a typical synthesis process for the CrN dendrites, 2 mmol of $CrCl_3$ and 8 mmol of $NaNH_2$ (with 2 mmol excessive) were ground together for 15 min by ball milling before put into an stainless-steel autoclave of 10-mL capacity. The autoclave was sealed and maintained at 250 °C for 4 h, then cooled to room temperature on standing. The black product was collected, rinsed with absolute ethanol and distilled water in sequence, and then dried under vacuum at 60 °C for 4 h.

The typical XRD pattern of the final product is shown in Figure 1. All the peaks can be indexed to the cubic rocksalt CrN with lattice constant $a = 4.143$ Å, which is consistent with the literature (JCPDS Card. No. 76-2494). No impurity peaks from Cr, Cr_2N, or Cr_2O_3 were found in the experimental range. Further evidence for the surface composition of the product can be obtained by XPS measurement. The binding energies of Cr $2p_{3/2}$, $2p_{1/2}$, and N 1s are 575.6, 585.4, and 396.4 eV, respectively, which also confirm the formation of cubic CrN.[3] The quantification of peaks gives a Cr:N ratio of 0.81:1.

TEM (Hitachi H-800), HRTEM (JEOL-2010) and FE-SEM (JEOL JSM-6700F) images of the product are shown in Figures 2 and 3, respectively. Figure 2a shows the typical TEM image of CrN with well-arrayed dendritic structures with lengths in the range of 400–600 nm and width of 30–40 nm. A few rather long dendritic crystals (Figure 2b) with length in the range of 3–4 μm also exist in the as-prepared product. More careful observation
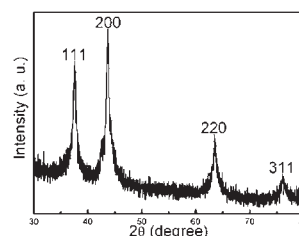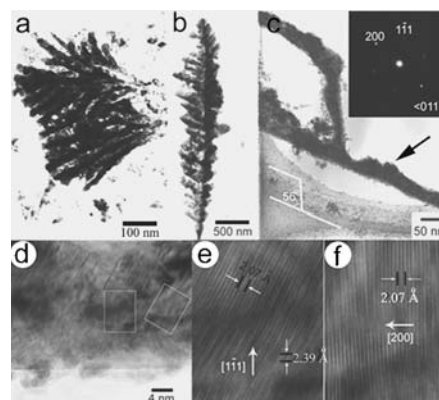

Figure 2. (a) TEM image of as-obtained CrN with well-arrayed dendritic structures. (b) TEM image of a rather long CrN dendrite. (c) TEM image with high magnification of one branch (the inset is SAED on the trunk). (d) HRTEM image of a CrN dendritic crystal. (e and f) Magnified HRTEM images of the parts of Figure 2d indicated by the boxes.
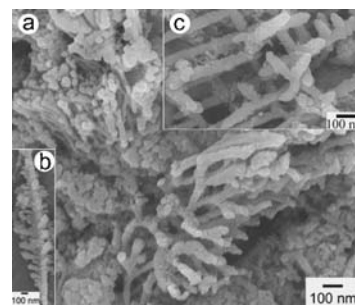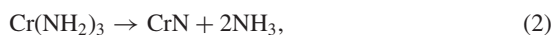

Figure 3. FE-SEM images of CrN with dendritic nanostructures.

of a further amplified image can be obtained from Figure 2c which reveals that the acute angle between the trunk and branch keeps around 56°. The corresponding SAED (inset of Figure 2c) recorded from the ⟨011⟩ zone axis confirms the single-crystalline

nature, and the diffraction spots can be indexed to the reflections of cubic CrN, which is consistent with the XRD pattern. Figure 2d is the HRTEM image of a branch, with the enlargements of the boxed regions shown in Figures 2e and 2f. From the HRTEM images, the lattice fringes can be clearly seen and indexed to the (111) and (200) planes of cubic CrN. It shows that the growth direction of the well-arrayed dendritic crystal is parallel to the (111) plane. Some edge dislocations and stacking faults are also found in the HRTEM images. The FE-SEM images (Figure 3) further reveal the typical dendritic structure of the as-obtained product, which are in good agreement with the corresponding TEM studies.

Our rapid solvent-free synthesis of cubic CrN at 250 °C is essentially based on the self-propagating reaction between $CrCl_3$ and $NaNH_2$ owing to the low melting point (210 °C) of $NaNH_2$. Previous research showed that $LiNH_2$ could react with a class of anhydrous transition-metal chlorides to form metal amides, which produced metal nitrides under the subsequent high-temperature pyrogenation.[4] In the present work, the first step in the mechanism is also that of metathetical exchange to generate NaCl and $Cr(NH_2)_3$, then $Cr(NH_2)_3$ was decomposed to CrN by the heat energy released by the upper reaction. The reactions involved here are as follows:

$$CrCl_3 + 3NaNH_2 \rightarrow Cr(NH_2)_3 + 3NaCl, \qquad (1)$$

$$Cr(NH_2)_3 \rightarrow CrN + 2NH_3, \qquad (2)$$

$$CrCl_3 + 3NaNH_2 \rightarrow CrN + 3NaCl + 2NH_3. \qquad (3)$$

According to free energy calculation, the reaction between $CrCl_3$ and $NaNH_2$, described as eq 3, is thermodynamically spontaneous ($\Delta_r G^o = -600.00 \, kJ/mol$) and highly exothermic ($\Delta_r H^o = -514.28 \, kJ/mol$).[5] The heat energy released rapidly results in a transiently high temperature and the molten by-product of NaCl, which is favorable to the formation and crystallization of CrN. The addition of excessive 2 mmol of $NaNH_2$ in the initial reagents is used to provide a higher supersaturation environment.

Herein, the vapor–liquid–solid (VLS) mechanism and the fluctuation of supersaturation were proposed to explain the growth of CrN dendrites. It is worth noting that there are droplets, which are inherent to the VLS mechanism, were found on the tip of some branches in the as-obtained product (shown in Figure 3a). This fact suggests that the VLS mechanism was dominant in the one-dimensional growth of CrN. At high supersaturation, the sublimation velocity is very big. In the higher supersaturation zone caused by fluctuation, the flange will occur on the 1-D trunk (shown in Figure 2c) because of fast growth.[6] Latent heat at the tip of the flange dissipates easier than that of flank. Since the growth velocity at the tip of the flange is quicker than that of flank, the flange grows into very small crystal to form the branch of dendritic crystal. This progress continues to grow the 3-D dendritic nanostructure.

To approve above mechanism, 1.5 mmol of NaCl diluent was added to the initial reagents to lower the supersaturation. The as-obtained product was confirmed to be cubic CrN by XRD and XPS; however, the TEM (Figure 4a) and FE-SEM (Figure 4b) studies demonstrate the growth of dendritic nanostructure that has been successfully restrained, and the product dominantly consist of whisker and whisker bundles as expected.

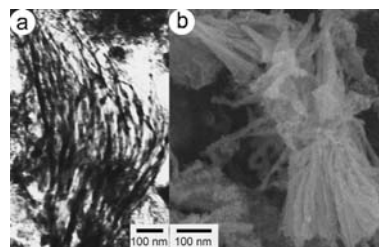Further study reveals that a higher temperature (>350 °C) or

Figure 4. (a) TEM image of as-obtained CrN whisker bundle dispersed in the ethanol. (b) FE-SEM image of a CrN whisker bundle without any dispersion treatment.

the excessive initial reagents is harmful to the growth of CrN dendrites. When the temperature is higher than 350 °C or the amount of $CrCl_3$ is more than 5 mmol with proportional increase of $NaNH_2$, relatively monodisperse CrN nanoparticles with average size of about 5 nm rather than dendrites were obtained. For directly tracing the whole reaction process, the reactions were run in an evacuated quartz tube furnace with a heating rate of 30 °C min^{-1} at 350 and 250 °C, respectively. Unlike the fast reaction with the character of thermal flash at 350 °C, the reagents smoldered first at 250 °C accompanied by an energy release, which ultimately ignited the strenuous reaction. It is reasonable to assume that the different reaction rate at different heat temperature is one of the most important factors in inducing the two distinct morphologies. Hence, milder and long-time conditions are in favor of the growth of dendrite.

In summary, by controlling the supersaturation CrN with novel dendritic and bundle-like nanostructures was successfully synthesized via the solvent-free reaction of $CrCl_3$ and $NaNH_2$ at 250 °C. The VLS mechanism and the fluctuation of supersaturation are likely to be responsible for the dendritic and bundle-like nanostructures. The appropriate conditions for the synthesis of dendritic CrN are also discussed here.

References
1 a) J. P. Xiao, Y. Xie, R. Tang, M. Chen, and X. B. Tian, *Adv. Mater.*, **13**, 1887 (2001). b) L. W. Yin, M. S. Li, Y. X. Liu, B. Xu, J. L. Sui, and Y. X. Qi, *Adv. Mater.*, **15**, 720 (2003). c) Y. J. Song, Y. Yang, C. J. Medforth, E. Pereira, A. K. Singh, H. F. Xu, Y. B. Jiang, C. J. Brinker, F. V. Swol, and J. A. Shelnutt, *J. Am. Chem. Soc.*, **126**, 635 (2004). d) Z. P. Zhang, X. Q. Shao, H. D. Yu, Y. B. Wang, and M. Y. Han, *Chem. Mater.*, **17**, 332 (2005).
2 a) M. D. Aguas, A. M. Nartowski, I. P. Parkin, M. MacKenzie, and A. J. Craven, *J. Mater. Chem.*, **8**, 1875 (1998). b) J. L. O. Loughlin, C. H. Wallace, M. S. Knox, and R. B. Kaner, *Inorg. Chem.*, **40**, 2240 (2001).
3 Z. D. Zhang, R. M. Liu, and Y. T. Qian, *Mater. Res. Bull.*, **37**, 1005 (2002).
4 I. P. Parkin and A. T. Rowley, *J. Mater. Chem.*, **5**, 909 (1995).
5 J. A. Dean, "Lange's Handbook of Chemistry," 13th ed., McGraw-Hill, New York (1985).
6 M. E. Glicksman and A. O. Lupulescu, *J. Cryst. Growth*, **264**, 541 (2004).